

# UCPO: Uncertainty-Aware Policy Optimization

Xianzhou Zeng<sup>1</sup>, Jing Huang<sup>2</sup>, Chunmei Xie<sup>1</sup>, Gongrui Nan<sup>1</sup>, Siye Chen<sup>1</sup>, Mengyu Lu<sup>1</sup>, Weiqi Xiong<sup>1</sup>, Qixuan Zhou<sup>1</sup>, Junhao Zhang<sup>2</sup>, Qiang Zhu<sup>2</sup>, Yadong Li<sup>1,†</sup>, Xingzhong Xu<sup>1</sup>

<sup>1</sup>Ant Group <sup>2</sup>Zhejiang University

{zengxianzhou.zxz, liyadong.lyd}@antgroup.com

## Abstract

The key to building trustworthy Large Language Models (LLMs) lies in endowing them with inherent uncertainty expression capabilities to mitigate the hallucinations that restrict their high-stakes applications. However, existing RL paradigms such as GRPO often suffer from Advantage Bias due to binary decision spaces and static uncertainty rewards, inducing either excessive conservatism or overconfidence. To tackle this challenge, this paper unveils the root causes of reward hacking and overconfidence in current RL paradigms incorporating uncertainty-based rewards, based on which we propose the **Un**Certainty-Aware Policy Optimization (UCPO) framework. UCPO employs Ternary Advantage Decoupling to separate and independently normalize deterministic and uncertain rollouts, thereby eliminating advantage bias. Furthermore, a Dynamic Uncertainty Reward Adjustment mechanism is introduced to calibrate uncertainty weights in real-time according to model evolution and instance difficulty. Experimental results in mathematical reasoning and general tasks demonstrate that UCPO effectively resolves the reward imbalance, significantly improving the reliability and calibration of the model beyond their knowledge boundaries.

## 1. Introduction

While Large Language Models (LLMs) excel in complex reasoning, their inherent hallucinations remain a critical barrier to high-stakes deployment (Huang et al., 2023; Cossio, 2025). Building trustworthy AI necessitates endowing models with uncertainty awareness, enabling them to recognize cognitive boundaries and express doubt when queries exceed their internal knowledge (Tonmoy et al., 2024).

To equip models with uncertainty awareness, existing research primarily follows two trajectories (Wen et al., 2025).

<sup>†</sup>Corresponding author.

<sup>1</sup><https://github.com/xzhouzeng/ucpo>

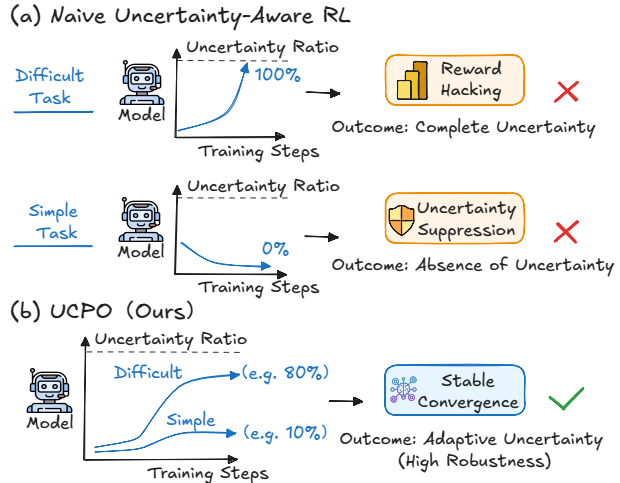


Figure 1. Illustration of reward imbalance in uncertainty alignment: static rewards trigger overconfidence or avoidance degeneracy, whereas UCPO stabilizes the policy through adaptive calibration.

The first employs Supervised Fine-Tuning (SFT) using instructional datasets with explicit abstention labels to facilitate imitation learning (Amayuelas et al., 2024; Kapoor et al., 2024). However, the high cost of data synthesis and the inability of static datasets to capture dynamic inference-time uncertainty limit its scalability. The second approach utilizes Reinforcement Learning (RL) by assigning fixed intermediate rewards (e.g., 0.5) to uncertain responses. While this method requires no additional annotation, its efficacy is highly sensitive to reward tuning (Wei et al., 2025; Ren et al., 2025). As shown in Figure 1-(a), this naive uncertainty-aware RL paradigm lacks robustness: static rewards cannot adapt to evolving model capabilities or varying task difficulties. In difficult tasks, models often succumb to reward hacking, resulting in avoidance degeneracy where risk is mitigated through excessive refusal. Conversely, in simpler tasks, subtle uncertainty signals are frequently overwhelmed by the high rewards of correct answers, resulting in overconfidence and the suppression of uncertainty cognition.

Addressing these challenges, this paper provides an in-depth analysis of the underlying mechanisms by which existing RL methods trigger reward hacking and overconfidence. We reveal that a fixed uncertainty reward mechanism leads to a

bias in the Advantage Function across different performance intervals: in high-performance regimes, models fail to learn uncertainty as the uncertainty advantage turns negative; in low-performance regimes, models lapse into reward hacking due to an overloaded uncertainty advantage. Building on these insights, we propose the Uncertainty-Aware Policy Optimization (UCPO) framework, which transcends the limitations of binary decision spaces to achieve a dynamic equilibrium among truthful, erroneous, and abstinent ternary responses. Specifically, UCPO comprises two synergistic components: Ternary Advantage Decoupling (TAD), which decomposes sampling paths into independent deterministic and uncertain channels and implements Independent Advantage Normalization to eliminate mutual interference between semantic signals; and Dynamic Uncertainty Reward Adjustment (DURA), which realigns reward weights in real-time based on the evolution of model capability and sample difficulty distribution, effectively mitigating policy drift caused by static reward imbalance.

Experimental results on Qwen3 (Yang et al., 2025) and Llama3.1 (Dubey et al., 2024) show that UCPO achieves stable convergence across varying task difficulties, as illustrated in Figure 1-(b). Evaluations in mathematical reasoning and general domains confirm that UCPO effectively reduces hallucinations while enhancing reliability and probability calibration at the model’s cognitive boundaries.

The contributions of this paper are summarized as follows:

- We analyze the mechanisms of advantage bias and static reward failure within uncertainty-aware reinforcement learning, identifying the root causes of overconfidence and avoidance degeneracy.
- By integrating TAD and DURA, UCPO establishes an adaptive RL paradigm for the trustworthy alignment of LLMs that eliminates the need for exhaustive reward hyperparameter tuning.
- Extensive experiments demonstrate UCPO’s efficacy in mitigating hallucinations and enhancing uncertainty expression across various tasks.

## 2. Preliminary

In this section, we first review the Group Relative Policy Optimization (GRPO) framework (Shao et al., 2024). Building on this, we delineate the Ternary Imbalance Problem inherent in the integration of uncertainty rewards within this framework.

### 2.1. Group Relative Policy Optimization

GRPO streamlines the reinforcement learning process by obviating the need for a separate value function. Instead of

estimating state values, it leverages the collective rewards of multiple outputs generated from the same prompt to derive a baseline for advantage estimation.

Specifically, for a given prompt  $q$ , the policy model  $\pi_\theta$  generates a group of  $G$  outputs  $\{o_1, o_2, \dots, o_G\}$ . In a standard binary setting, each rollout  $o_i$  receives a reward  $r_i \in \{r_{\text{wrong}}, r_{\text{right}}\}$ . The advantage  $\hat{A}_{i,t}$  is computed via group-relative normalization:

$$\hat{A}_{i,t} = \frac{r_i - \text{mean}(\mathbf{r})}{\text{std}(\mathbf{r})} \quad (1)$$

where  $\mathbf{r} = [r_1, r_2, \dots, r_G]$ . This ensures  $\sum_{i=1}^G \hat{A}_{i,t} = 0$ , creating a zero-sum gradient signal. Building upon this advantage estimate, the policy is updated by maximizing the GRPO objective function  $\mathcal{J}_{\text{GRPO}}(\theta)$ :

$$\mathcal{J}_{\text{GRPO}}(\theta) = \mathbb{E} \left[ \frac{1}{G} \sum_{i=1}^G \frac{1}{|o_i|} \sum_{t=1}^{|o_i|} \left( \min \left( r_{i,t}(\theta) \hat{A}_{i,t}, \text{clip}(r_{i,t}(\theta), 1 - \varepsilon, 1 + \varepsilon) \hat{A}_{i,t} \right) - \beta D_{\text{KL}}(\pi_\theta \| \pi_{\text{ref}}) \right) \right] \quad (2)$$

where  $r_{i,t}(\theta) = \pi_\theta(o_{i,t}|q, o_{i,<t}) / \pi_{\theta_{\text{old}}}(o_{i,t}|q, o_{i,<t})$  is the probability ratio between the current and old policies.

### 2.2. The Ternary Imbalance Problem

To equip the model with the ability to express uncertainty, an intuitive extension is to introduce an uncertain category into the original reward space. This category is assigned a median reward value  $r_{\text{uncertain}}$  (hereafter  $r_u$ ), such that  $r_{\text{wrong}} < r_u < r_{\text{right}}$  (set as 0, 0.8, and 1 respectively in Fig. 2). We refer to this direct integration of uncertainty rewards within the GRPO framework as GRPO-UC.

The transition from a binary to a ternary reward modeling introduces a fundamental optimization bias. We visualize this via ternary plots in Figure 2, analyzing two key metrics of GRPO-UC across diverse sample distributions: the normalized advantage of uncertain rollouts and the Net Right Advantage (defined as the difference between the aggregated advantages of right rollouts and uncertain rollouts). Our analysis reveals that the advantage signal for uncertain rollouts is highly sensitive to the model’s evolving capability, triggering two distinct failure modes:

- **Uncertainty Suppression in High-Performance Regimes:** As the model gains proficiency, the advantage of uncertain rollouts ( $A_{\text{uncertain}}$ ) turns negative (red region, Fig 2.a). This illustrates Majoritarian Suppression, where the global average performance penalizes locally rational, conservative decisions. Rather

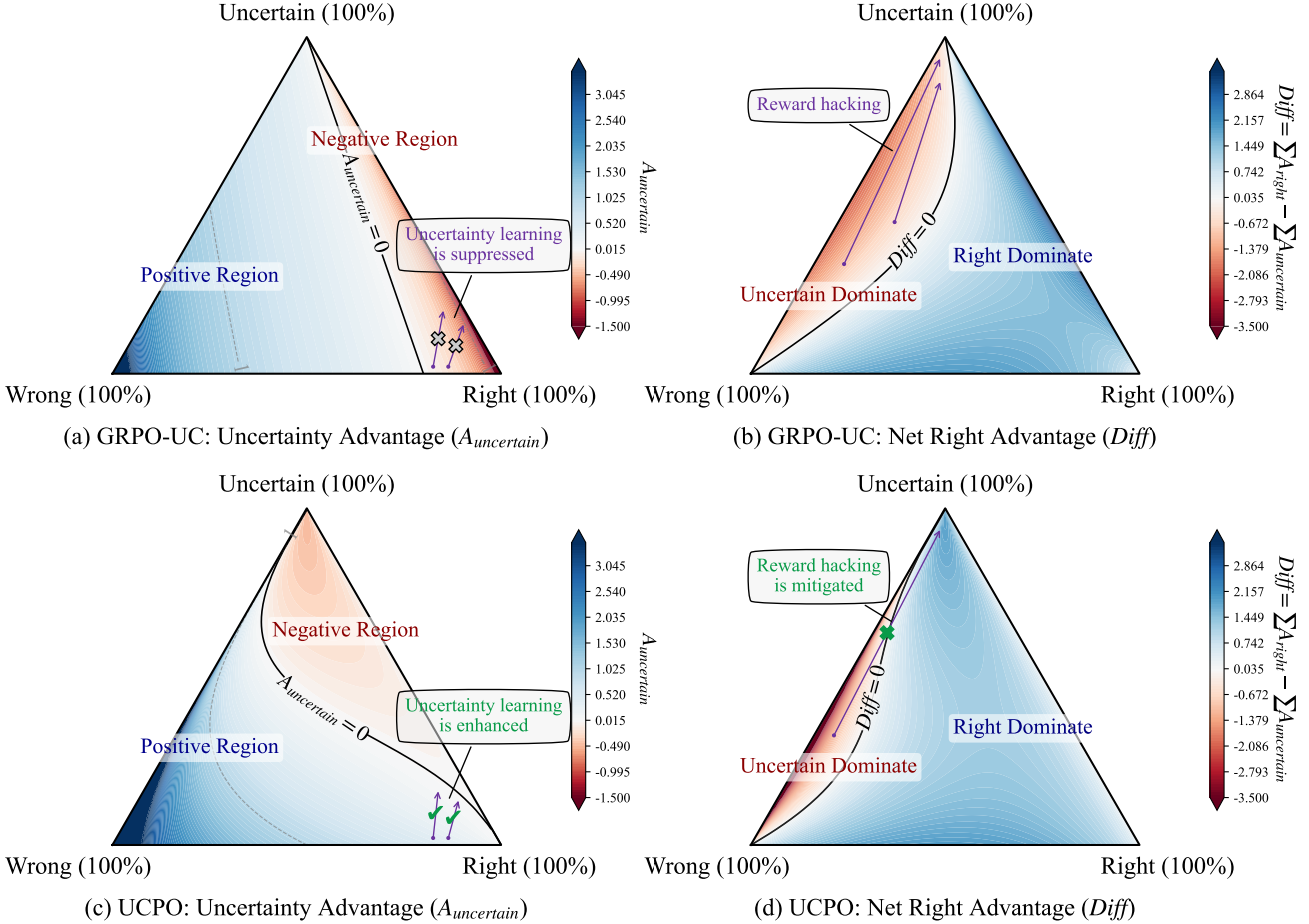


Figure 2. The Ternary Imbalance Problem in GRPO-UC (a-b) contrasted with the balanced advantage distribution in UCPO (c-d). Each point in the ternary plots represents a specific combination of Right, Wrong, and Uncertain proportions within a group of  $G$  outputs.

than being punished for errors, the model is penalized because its cautious choice yields returns below the group’s high expectations, compelling overconfidence on ambiguous samples.

- **Reward Hacking in Low-Performance Regimes:** In low-performance regimes or on high-difficulty tasks, the total advantage of uncertain rollouts dominates the policy gradient (red region, Fig 2.b). This triggers Reward Hacking, where the model identifies claiming uncertainty as a shortcut to maximize rewards without performing complex reasoning. Such behavior leads to Mode Collapse, where the model defaults to uncertainty for all inputs, stifling the incentive to learn discriminative features required for correct predictions.

The proposed UCPO breaks this ternary imbalance by restructuring the uncertain reward mechanism (Fig 2.c, d). By decoupling uncertainty rewards from global performance averages, UCPO maintains a positive advantage for uncertain rollouts in high-performance regimes where hallucinations

persist, effectively preventing majoritarian suppression. Simultaneously, in low-performance regimes, it balances the gradient flow so that the uncertainty advantage does not dominate the optimization path toward an all-uncertainty policy, avoiding reward hacking and maintaining optimization pressure for learning discriminative features.

### 3. Method

To overcome the limitations of static uncertain reward modeling, we propose Uncertainty-Aware Policy Optimization (UCPO). UCPO replaces traditional binary feedback with a ternary reward modeling system that distinguishes among right, wrong, and uncertain responses. Specifically, UCPO redefines the advantage estimation  $\hat{A}_{i,t}$  through two synergistic mechanisms, as illustrated in Figure 3.

#### 3.1. Ternary Advantage Decoupling (TAD)

To prevent uncertainty signals from being overshadowed by high-reward right answers, UCPO employs TAD to

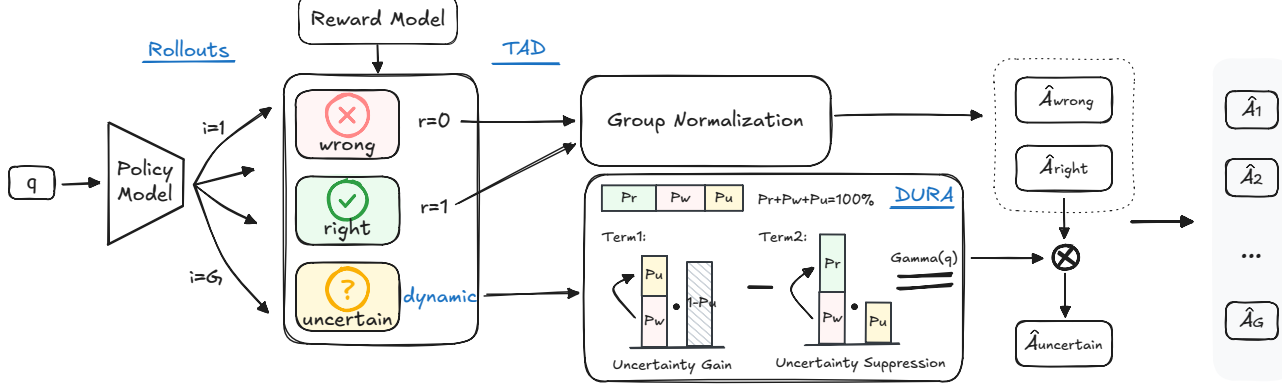


Figure 3. Architecture of the UCPO Framework.

isolate deterministic and uncertain signals, thereby eliminating semantic interference during advantage estimation. We partition the group of  $G$  rollouts into a deterministic set  $\mathcal{S}_{det} = \{o \in \text{Right} \cup \text{Wrong}\}$  and an uncertainty set  $\mathcal{S}_{unc} = \{o \in \text{Uncertain}\}$ .

The advantage  $\hat{A}_{i,t}$  is computed through two independent channels:

- **Deterministic Channel** ( $o_i \in \mathcal{S}_{det}$ ): The advantage is calculated strictly within the deterministic subset to maintain the gradient of correctness:

$$\hat{A}_{i,t}^{det} = \frac{r_i - \text{mean}(\mathbf{r}_{det})}{\text{std}(\mathbf{r}_{det}) + \epsilon} \quad (3)$$

Here,  $\mathbf{r}_{det} = \{r_j \mid o_j \in \text{Right} \cup \text{Wrong}\}$  isolates core knowledge acquisition from metacognitive learning. In this channel, correct paths yield positive reinforcement ( $\hat{A}_{right} > 0$ ), while erroneous paths provide corrective penalties ( $\hat{A}_{wrong} < 0$ ) to suppress hallucinations.

- **Uncertainty Channel** ( $o_i \in \mathcal{S}_{unc}$ ): The advantage for expressing uncertainty is defined as a dynamic projection of the right-sample advantage:

$$\hat{A}_{i,t}^{unc} = \gamma(q) \cdot \hat{A}_{right} \quad (4)$$

By adopting  $\hat{A}_{right}$  as a performance anchor, the incentive for uncertainty is dynamically scaled relative to the model's current peak reasoning capability. This anchoring prevents the signal suppression inherent in global normalization, where high right-sample density often forces uncertainty advantages into negative values, inadvertently penalizing honest doubt. By projecting  $\hat{A}_{right}$  through the gain  $\gamma(q)$ , UCPO maintains a positive gradient to curb hallucinations during high-error phases. The gain coefficient  $\gamma(q)$ , generated by the DURA module, adaptively modulates this signal.

Note that if  $\mathcal{S}_{det}$  lacks either correct or incorrect rollouts, we filter these samples, a process defined as Non-Ternary Filtering (NTF). Analogous to the zero-advantage setting in standard GRPO for all-correct or all-incorrect groups, NTF effectively discards such samples to maintain training stability during extreme performance phases.

By decoupling these channels, TAD treats the expression of uncertainty as a distinct, legitimate cognitive state, preventing the model from treating it as a shortcut to bypass difficult reasoning.

### 3.2. Dynamic Uncertainty Reward Adjustment (DURA)

To maintain a stable ternary equilibrium, we introduce DURA to adaptively modulate the gain coefficient  $\gamma(q)$ . DURA monitors the model's real-time error rates and confidence levels to prevent both overconfidence and avoidance degeneracy through a dual-term formulation:

$$\gamma(q) = \underbrace{\left( \frac{P_w}{P_u + P_w + \epsilon} \right) (1 - P_u)}_{\text{Term 1: Uncertainty Gain}} - w \cdot \underbrace{\left( \frac{P_r}{P_r + P_w + \epsilon} \right) P_u}_{\text{Term 2: Uncertainty Suppression}} \quad (5)$$

where  $P_r, P_w, P_u$  denote the ratios of Right, Wrong, and Uncertain rollouts within a group, respectively, and  $w = 1$  is a weighting constant. The mechanism functions as follows:

- **Uncertainty Gain (Term 1):** This term amplifies the incentive for uncertainty when the model's error-to-uncertainty ratio is high. By scaling with  $(1 - P_u)$ , it encourages the transition from hallucinations to honest doubt while preventing the policy from saturating in total avoidance.

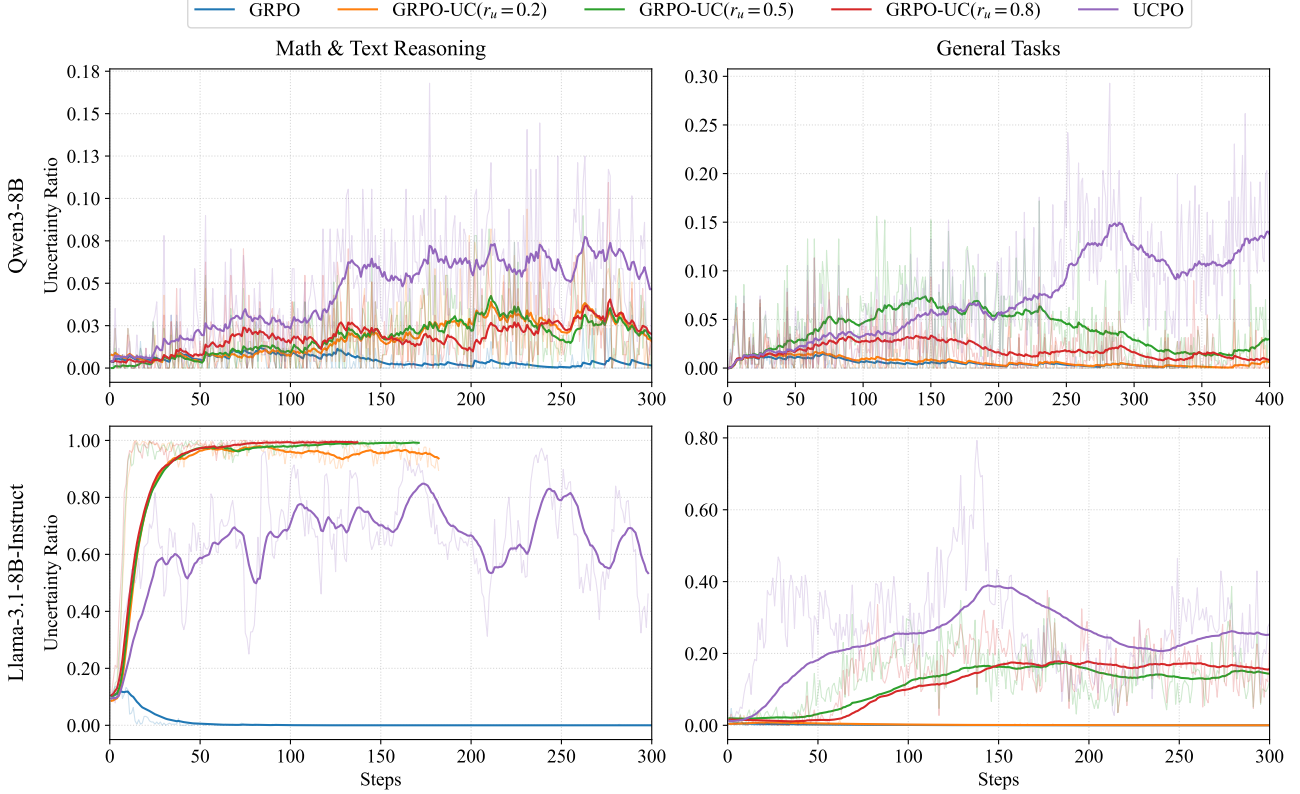


Figure 4. Evolution of the uncertainty ratio over training steps, comparing baseline GRPO, the proposed UCPO, and GRPO-UC variants with different reward coefficients  $r_u$ .

- **Uncertainty Suppression (Term 2):** As the model’s proficiency improves ( $P_r$  increases), this term penalizes unnecessary avoidance. It effectively raises the competitive bar for choosing the uncertainty path, pushing the model to commit to a definitive correct answer when it has the capacity to do so, rather than defaulting to a safe but uninformative response.

DURA dynamically balances these terms, making the uncertainty channel a regulated buffer: it suppresses hallucinations early in training while driving the model toward deterministic accuracy as reasoning improves. Notably, in low-resource scenarios with limited rollouts, the gain estimation suffers from high variance and reduced dynamic range. To address this, we propose Extensions for Low-Resource Scenarios, including batch-level smoothing and non-linear mapping; see the supplementary material for details.

## 4. Experiments

### 4.1. Experimental Settings

**Datasets and evaluation metrics.** This study evaluates cognitive boundaries and hallucination mitigation through two task paradigms. The first, free-form Math & Text Rea-

soning, employs DAPO-Math-17k (Yu et al., 2025) for training and assesses performance on AIME24 (AIM, 2024), AMC (LI et al., 2024), MATH500 (Lightman et al., 2023), Minerva (Lewkowycz et al., 2022) and Olympiad Bench (He et al., 2024). The second, constrained-choice General Tasks, uses MMLU-Redux2 (Gema et al., 2025) (with 1,000 instances partitioned for testing and the remainder for training) and GPQA-Diamond (Rein et al., 2024) to scrutinize overconfidence under compelled-choice scenarios. Model responses are categorized as Accuracy (*Acc*), Hallucination (*Hal*), or Uncertainty (*Unc*). Following KnowRL (Ren et al., 2025), we employ two primary metrics: Precision on Answered Questions (PAQ), defined as  $Acc/(Acc + Hal)$ , to measure the reliability of non-uncertain outputs; and the F1 Score, which balances truthfulness and informativeness by penalizing both erroneous assertions and excessive conservatism.

**Models and Baselines.** To assess generalizability, Qwen3-8B and Llama-3.1-8B-Instruct are selected as backbone models. Comparative baselines include the original Baseline, prompt-based uncertainty-aware guidance (Prompt-UC), and standard GRPO utilizing binary rewards ( $Right = 1, Wrong = 0$ ). Additionally, GRPO-UC is included as

Table 1. Performance on Math & Text Reasoning tasks.  $\dagger$  denotes the GRPO-UC reward coefficients  $r_u \in \{0.2, 0.5, 0.8\}$ .

Methods	AIME24		AMC		MATH500		Minerva		Olympiad Bench		Average	
	PAQ	F1	PAQ	F1	PAQ	F1	PAQ	F1	PAQ	F1	PAQ	F1
<b>Qwen3-8B</b>												
Baseline	73.33	73.33	91.57	<u>91.57</u>	96.80	<b>96.80</b>	45.96	45.96	69.63	<b>69.63</b>	75.46	75.46
Prompt-UC	73.33	73.33	89.02	88.48	95.80	95.80	<b>49.43</b>	<b>48.60</b>	<u>71.49</u>	<u>70.47</u>	75.82	75.34
GRPO	77.01	75.71	88.35	88.35	96.46	96.36	47.18	46.62	69.22	68.25	75.64	75.06
GRPO-UC $^{\dagger 0.2}$	<u>83.75</u>	<b>78.82</b>	88.98	88.26	96.31	95.99	48.60	47.62	70.68	68.35	<u>77.66</u>	<u>75.81</u>
GRPO-UC $^{\dagger 0.5}$	80.00	75.29	90.00	88.34	96.24	95.95	46.32	45.51	70.84	68.64	76.68	74.75
GRPO-UC $^{\dagger 0.8}$	72.41	71.19	<b>95.06</b>	<b>93.90</b>	96.20	96.20	47.55	46.93	70.68	69.24	76.38	75.49
UCPO	<b>86.11</b>	76.54	<u>91.95</u>	89.48	<b>97.28</b>	96.40	49.15	<u>47.63</u>	<b>73.67</b>	69.42	<b>79.63</b>	<b>75.90</b>
<b>Llama-3.1-8B-Instruct</b>												
Baseline	3.33	<u>3.33</u>	15.66	15.66	45.80	45.80	15.81	15.81	14.96	14.96	19.11	19.11
Prompt-UC	<b>6.98</b>	<b>6.82</b>	19.74	19.09	47.32	<u>46.34</u>	16.54	16.04	17.45	<u>16.61</u>	21.61	<u>20.98</u>
GRPO	3.33	3.33	20.08	<u>20.08</u>	43.96	43.95	18.16	<u>18.15</u>	14.76	14.74	20.06	20.05
GRPO-UC $^{\dagger 0.2}$	3.85	2.82	11.80	9.27	40.98	33.60	19.88	<u>11.50</u>	13.58	9.38	18.02	13.31
GRPO-UC $^{\dagger 0.5}$	0.00	0.00	<u>21.43</u>	6.19	<u>57.61</u>	25.53	<b>26.16</b>	9.11	<u>19.28</u>	4.22	<u>24.90</u>	9.01
GRPO-UC $^{\dagger 0.8}$	0.00	0.00	15.79	2.24	56.61	12.67	<u>25.00</u>	4.87	12.90	1.49	22.06	4.25
UCPO	<u>5.13</u>	3.10	<b>28.12</b>	<b>22.00</b>	<b>60.95</b>	<b>51.95</b>	22.50	<b>18.48</b>	<b>25.56</b>	<b>17.69</b>	<b>28.45</b>	<b>22.65</b>

Table 2. Performance on General Tasks.  $\dagger$  denotes the GRPO-UC reward coefficients  $r_u \in \{0.2, 0.5, 0.8\}$ .

Methods	GPQA-Diamond		MMLU-Redux2		Average	
	PAQ	F1	PAQ	F1	PAQ	F1
<b>Qwen3-8B</b>						
Baseline	56.57	56.57	87.20	87.20	71.88	71.88
Prompt-UC	56.84	55.67	87.08	86.33	71.96	71.00
GRPO	59.35	58.79	87.62	87.21	73.48	73.00
GRPO-UC $^{\dagger 0.2}$	60.25	<u>59.06</u>	88.13	<b>87.61</b>	74.19	<u>73.33</u>
GRPO-UC $^{\dagger 0.5}$	<u>65.09</u>	58.65	<u>88.82</u>	86.61	<u>76.96</u>	72.63
GRPO-UC $^{\dagger 0.8}$	64.00	<b>60.05</b>	88.51	<u>87.51</u>	76.26	<b>73.78</b>
UCPO	<b>67.70</b>	56.16	<b>91.67</b>	85.42	<b>79.68</b>	70.79
<b>Llama-3.1-8B-Instruct</b>						
Baseline	22.56	22.56	65.17	65.17	43.86	43.86
Prompt-UC	23.28	22.74	68.02	67.41	45.65	45.07
GRPO	27.27	27.27	71.23	71.23	49.25	<u>49.25</u>
GRPO-UC $^{\dagger 0.2}$	29.46	<b>29.46</b>	72.47	<b>72.47</b>	50.96	<b>50.96</b>
GRPO-UC $^{\dagger 0.5}$	34.21	18.98	<u>78.89</u>	<u>71.51</u>	<u>56.55</u>	45.25
GRPO-UC $^{\dagger 0.8}$	34.32	<u>19.52</u>	76.99	69.78	55.66	44.65
UCPO	<b>36.02</b>	17.18	<b>81.13</b>	69.03	<b>58.58</b>	43.10

a representative uncertainty learning strategy, employing fixed uncertainty rewards ( $r_u \in \{0.2, 0.5, 0.8\}$ ) to highlight advantage bias and training instability in ternary decision spaces.

**Training and Evaluation Details.** All experiments are conducted on a cluster of 8 A100 GPUs with a sampling group size  $G = 8$  for reinforcement learning. During the evaluation phase, the decoding temperature is set to 0.6. To ensure statistical reliability, all metrics are reported as the

average performance across three independent responses generated for each instance.

## 4.2. Analysis of Training Dynamics

To investigate the underlying mechanisms of uncertainty learning, we analyze the evolution of the uncertainty ratio across diverse models and tasks. As illustrated in Figure 4, standard GRPO consistently maintains a near-zero uncertainty ratio, as its binary reward structure (*Right/Wrong*) provides no incentive for expressing doubt, resulting in persistent overconfidence. While the GRPO-UC variant attempts to address this with a fixed uncertainty reward ( $r_u$ ), it proves highly brittle across varying task difficulties. On high-accuracy tasks (e.g., Qwen3-8B on Math & Text Reasoning), the fixed reward is insufficient to overcome the model’s inherent bias toward assertion, causing the uncertainty ratio to fluctuate near 0%. Conversely, on low-accuracy tasks (e.g., Llama-3.1-8B-Instruct on Math & Text Reasoning), a high fixed reward ( $r_u \geq 0.5$ ) triggers reward hacking, where the model prematurely abandons the exploration of correct reasoning paths in favor of guaranteed uncertainty rewards. This leads to a catastrophic collapse, with the uncertainty ratio surging to 100%.

These results indicate that UCPO effectively prevents avoidance degeneracy in complex tasks while eliciting honest expressions in simpler ones. By converting hallucinations into uncertainty without sacrificing proactive problem-solving, UCPO maintains an optimal trade-off between truthfulness and informativeness across varying task difficulties and model capacities. Detailed analyses of PAQ and F1 score

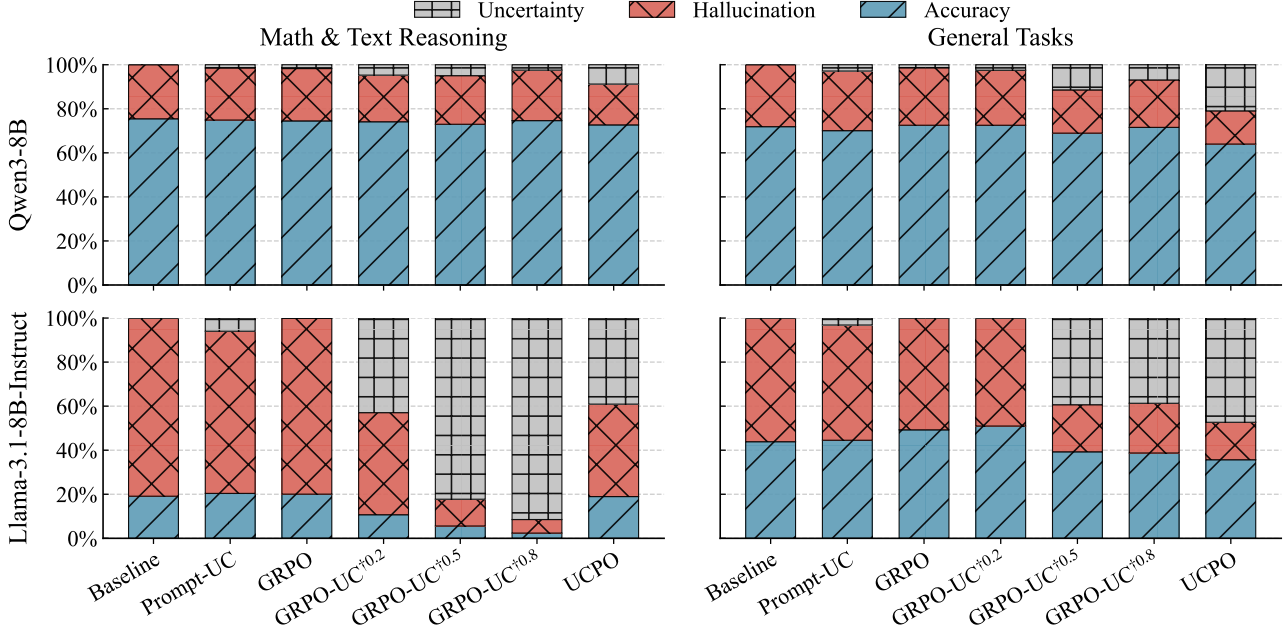


Figure 5. Aggregated distribution of Accuracy, Hallucination and Uncertainty across different alignment methods. Proportions are averaged over all datasets independently within the Math & Text Reasoning and General Tasks domains.

evolution relative to training steps and uncertainty ratios are provided in the Supplementary Material.

### 4.3. Main Results

Table 1 and Table 2 present the performance across math-reasoning and general knowledge tasks, while Figure 5 visualizes the corresponding response category distributions averaged independently within each task domain. Several key findings emerge:

**Calibration of Factual Reliability.** UCPO consistently achieves the highest Average PAQ across all evaluated domains. Specifically, in Math & Text Reasoning tasks, UCPO reaches a PAQ of 79.63% on Qwen3-8B and 28.45% on Llama-3.1-8B-Instruct. In General Tasks, it similarly leads with 79.68% and 58.58% for the respective models. As illustrated in Figure 5, this performance gain is primarily driven by the strategic conversion of hallucinations (red) into honest uncertainty expressions (gray). Unlike standard GRPO, which lacks a mechanism to penalize overconfident erroneous assertions, UCPO ensures that the model’s factual commitments are more reliable. This demonstrates an optimized trade-off between truthfulness and informativeness, effectively mitigating the risk of misinformation.

**Resolution of Fixed-Reward Brittleness.** A comparative analysis highlights a fundamental failure mode in the GRPO-UC baselines: extreme sensitivity to the fixed re-

ward  $r_u$ . While specific static rewards may yield balanced results for isolated datasets, they fail to generalize across varying difficulty gradients and task types. For instance, on Llama-3.1-8B-Instruct, a high  $r_u \geq 0.5$  in Math & Text Reasoning tasks inevitably triggers reward hacking, where the model bypasses the cognitive cost of reasoning in favor of guaranteed uncertainty rewards, leading to a catastrophic collapse in F1 scores (Notably, while uncertainty may converge to 100% during training, the test set ratio might not reach the same level due to the lack of perfect identical distribution, though it remains significantly high despite the distribution shift.). Conversely, in General Tasks, a lower  $r_u = 0.2$  results in the suppression of uncertainty learning; the weak incentive fails to encourage the model to acknowledge its knowledge boundaries, leaving it prone to random guessing and severe hallucinations. UCPO’s dynamic mechanism addresses these issues by preventing avoidance degeneracy in complex reasoning while eliciting honest expressions in general knowledge tasks, thereby maintaining robust problem-solving utility.

### 4.4. Ablation Study

To quantify each component’s contribution in UCPO, we conduct ablation studies on Llama-3.1-8B-Instruct (Table 3). Non-Ternary Filtering (NTF) refers to filtering out samples missing either correct or incorrect rollouts, as defined in the main text, while Low-Resource Extensions (LRE) are detailed in the supplementary material.

Table 3. Ablation study results on the Llama-3.1-8B-Instruct model. We evaluate the contribution of Ternary Advantage Decoupling (TAD), Dynamic Uncertainty Reward Adjustment (DURA), Non-Ternary Filtering (NTF), and Low-Resource Extensions (LRE).

TAD	DURA	NTF	LRE	Math & Text Reasoning			General Tasks		
				Uncertainty	PAQ	F1	Uncertainty	PAQ	F1
✗	✓	✓	✓	50.33	22.56	16.21	12.40	51.17	48.63
✓	✗	✓	✓	79.91	35.22	13.16	80.31	58.96	23.41
✓	✓	✗	✓	37.96	28.51	22.93	43.38	55.68	43.05
✓	✓	✓	✗	43.19	27.83	21.12	52.95	57.38	39.99
✓	✓	✓	✓	39.09	28.45	22.65	47.33	58.58	43.10

Removing Ternary Advantage Decoupling (TAD) significantly degrades PAQ; specifically in simpler tasks, the absence of decoupling allows deterministic gradients to overshadow subtle calibration signals, hindering the acquisition of effective uncertainty representations. Regarding the reward mechanism, omitting DURA leads to a performance collapse across both domains as the model over-optimizes for uncertainty rewards (a reward-hacking surge to  $\sim 80\%$  uncertainty). Moreover, the exclusion of Non-Ternary Filtering (NTF) induces training fluctuations and suboptimal convergence, whereas its inclusion, alongside Low-Resource Extensions (LRE), consistently yields higher F1 and PAQ scores by providing the necessary robustness for calibration under data constraints. These findings are further corroborated by the training trajectories in Figure 9 (Appendix), highlighting the synergistic effect of these modules in balancing accuracy and metacognitive calibration.

## 5. Related Work

### 5.1. Reinforcement Learning

Reinforcement Learning (RL) has emerged as the cornerstone paradigm for aligning Large Language Models and enhancing their multi-step reasoning capabilities (Li et al., 2025; Zhang et al., 2025). Within this landscape, GRPO represents a significant milestone; by introducing a critic-free architecture and group-relative normalization, it substantially reduces training variance and accelerates convergence (Shao et al., 2024; Guo et al., 2025). Building upon this foundation, subsequent studies such as Dr.GRPO (Liu et al., 2025a), DAPO (Yu et al., 2025), and LitePPO (Liu et al., 2025b) have further refined training stability through sophisticated sampling strategies, clipping mechanisms, and loss function optimizations. Meanwhile, PSR-NSR (Zhu et al., 2025) and NGRPO (Nan et al., 2025) explore the exploitation of negative samples to extract meaningful learning signals from erroneous responses. Diverging from these approaches, our proposed UCPO introduces uncertainty modeling to prevent the model from compulsive fitting of incomprehensible error signals, thereby effectively suppressing the emergence of hallucinations during the training process.

### 5.2. Uncertainty-aware Learning in LLMs

Current LLMs frequently exhibit factual hallucinations, largely due to underdeveloped refusal mechanisms (Wen et al., 2025; Madhusudhan et al., 2025; Kirichenko et al., 2025). To empower models to articulate uncertainty, early research primarily utilized uncertainty-guided prompts or strategies to induce verbalized confidence for calibration (Slobodkin et al., 2023; Tian et al., 2023). Moving further, the Supervised Fine-Tuning paradigm introduced specialized datasets with uncertainty annotations to map knowledge boundaries (Amayuelas et al., 2024; Kapoor et al., 2024; Cheng et al., 2024). While fine-tuning helps identify unanswerable queries, it is constrained by high labeling costs and an inability to capture a model’s internal limits. Recent RL-based reasoning advances have reduced supervision needs, but binary rewards often encourage overconfident guessing over honest uncertainty (Kalai et al., 2025; Yao et al., 2025). To mitigate this, TruthRL (Wei et al., 2025) and KnowRL (Ren et al., 2025) treat uncertain states as fixed intermediate reward values to guide the model toward exploring its knowledge limits. Despite their success in specific tasks, their hyperparameter sensitivity often triggers an imbalance between over-refusal and hallucination. Unlike fixed-reward methods, UCPO dynamically adjusts uncertainty rewards to ensure robust learning of uncertainty expressions across diverse tasks.

## 6. Conclusion

This paper presents UCPO, a reinforcement learning framework designed to empower LLMs to express uncertainty when encountering unknown queries. By implementing Ternary Advantage Decoupling and Dynamic Uncertainty Reward Adjustment, UCPO resolves the gradient interference and reward hacking inherent in naive methods, achieving stable and effective uncertainty learning. A remaining limitation is that the distribution ratios of different rollout types potentially influence uncertainty learning, a phenomenon observed in our experiments but not fully explored. Future work will investigate the specific impact of ternary signal distributions on training dynamics and explore more effective balancing strategies.

## References

AIME problems and solutions, 2024. URL [https://artofproblemsolving.com/wiki/index.php/AIME\\_Problems\\_and\\_Solutions](https://artofproblemsolving.com/wiki/index.php/AIME_Problems_and_Solutions).

Amayuelas, A., Wong, K., Pan, L., Chen, W., and Wang, W. Y. Knowledge of knowledge: Exploring known-unknowns uncertainty with large language models. In *Findings of the Association for Computational Linguistics: ACL 2024*, pp. 6416–6432, 2024.

Cheng, Q., Sun, T., Liu, X., Zhang, W., Yin, Z., Li, S., Li, L., He, Z., Chen, K., and Qiu, X. Can ai assistants know what they don't know? *arXiv preprint arXiv:2401.13275*, 2024.

Cossio, M. A comprehensive taxonomy of hallucinations in large language models, 2025. URL <https://arxiv.org/abs/2508.01781>.

Dubey, A., Jauhri, A., Pandey, A., Kadian, A., Al-Dahle, A., Letman, A., Mathur, A., Schelten, A., Yang, A., Fan, A., et al. The llama 3 herd of models. *arXiv e-prints*, pp. arXiv–2407, 2024.

Gema, A. P., Leang, J. O. J., Hong, G., Devoto, A., Mancino, A. C. M., Saxena, R., He, X., Zhao, Y., Du, X., Madani, M. R. G., et al. Are we done with mmlu? In *Proceedings of the 2025 Conference of the Nations of the Americas Chapter of the Association for Computational Linguistics: Human Language Technologies (Volume 1: Long Papers)*, pp. 5069–5096, 2025.

Guo, D., Yang, D., Zhang, H., Song, J., Zhang, R., Xu, R., Zhu, Q., Ma, S., Wang, P., Bi, X., et al. Deepseek-r1: Incentivizing reasoning capability in llms via reinforcement learning. *arXiv preprint arXiv:2501.12948*, 2025.

He, C., Luo, R., Bai, Y., Hu, S., Thai, Z., Shen, J., Hu, J., Han, X., Huang, Y., Zhang, Y., et al. Olympiadbench: A challenging benchmark for promoting agi with olympiad-level bilingual multimodal scientific problems. In *Proceedings of the 62nd Annual Meeting of the Association for Computational Linguistics (Volume 1: Long Papers)*, pp. 3828–3850, 2024.

Huang, L., Yu, W., Ma, W., Zhong, W., Feng, Z., Wang, H., Chen, Q., Peng, W., Feng, X., Qin, B., and Liu, T. A survey on hallucination in large language models: Principles, taxonomy, challenges, and open questions. *ArXiv*, abs/2311.05232, 2023.

Kalai, A. T., Nachum, O., Vempala, S. S., and Zhang, E. Why language models hallucinate. *arXiv preprint arXiv:2509.04664*, 2025.

Kapoor, S., Gruver, N., Roberts, M., Collins, K., Pal, A., Bhatt, U., Weller, A., Dooley, S., Goldblum, M., and Wilson, A. G. Large language models must be taught to know what they don't know. *Advances in Neural Information Processing Systems*, 37:85932–85972, 2024.

Kirichenko, P., Ibrahim, M., Chaudhuri, K., and Bell, S. J. Abstentionbench: Reasoning llms fail on unanswerable questions. *arXiv preprint arXiv:2506.09038*, 2025.

Lewkowycz, A., Andreassen, A., Dohan, D., Dyer, E., Michalewski, H., Ramasesh, V., Sloane, A., Anil, C., Schlag, I., Gutman-Solo, T., et al. Solving quantitative reasoning problems with language models. *Advances in neural information processing systems*, 35:3843–3857, 2022.

LI, J., Beeching, E., Tunstall, L., Lipkin, B., Solotskyi, R., Huang, S. C., Rasul, K., Yu, L., Jiang, A., Shen, Z., Qin, Z., Dong, B., Zhou, L., Fleureau, Y., Lample, G., and Polu, S. Numinamath. [<https://huggingface.co/AI-MO/NuminaMath-CoT>] ([https://github.com/project-numina/aimo-progress-prize/blob/main/report/numina\\_dataset.pdf](https://github.com/project-numina/aimo-progress-prize/blob/main/report/numina_dataset.pdf)), 2024.

Li, Z.-Z., Zhang, D., Zhang, M.-L., Zhang, J., Liu, Z., Yao, Y., Xu, H., Zheng, J., Wang, P.-J., Chen, X., et al. From system 1 to system 2: A survey of reasoning large language models. *arXiv preprint arXiv:2502.17419*, 2025.

Lightman, H., Kosaraju, V., Burda, Y., Edwards, H., Baker, B., Lee, T., Leike, J., Schulman, J., Sutskever, I., and Cobbe, K. Let's verify step by step. In *The Twelfth International Conference on Learning Representations*, 2023.

Liu, Z., Chen, C., Li, W., Qi, P., Pang, T., Du, C., Lee, W. S., and Lin, M. Understanding r1-zero-like training: A critical perspective. *arXiv preprint arXiv:2503.20783*, 2025a.

Liu, Z., Liu, J., He, Y., Wang, W., Liu, J., Pan, L., Hu, X., Xiong, S., Huang, J., Hu, J., et al. Part i: Tricks or traps? a deep dive into rl for llm reasoning. *arXiv preprint arXiv:2508.08221*, 2025b.

Madhusudhan, N., Madhusudhan, S. T., Yadav, V., and Hasemi, M. Do llms know when to not answer? investigating abstention abilities of large language models. In *Proceedings of the 31st International Conference on Computational Linguistics*, pp. 9329–9345, 2025.

Nan, G., Chen, S., Huang, J., Lu, M., Wang, D., Xie, C., Xiong, W., Zeng, X., Zhou, Q., Li, Y., et al. Ngrpo: Negative-enhanced group relative policy optimization. *arXiv preprint arXiv:2509.18851*, 2025.

Rein, D., Hou, B. L., Stickland, A. C., Petty, J., Pang, R. Y., Dirani, J., Michael, J., and Bowman, S. R. Gpqa: A graduate-level google-proof q&a benchmark. In *First Conference on Language Modeling*, 2024.

Ren, B., Qiao, S., Zheng, D., Chen, H., and Zhang, N. Knowrl: Exploring knowledgeable reinforcement learning for factuality. *arXiv preprint arXiv:2506.19807*, 2025.

Shao, Z., Wang, P., Zhu, Q., Xu, R., Song, J., Bi, X., Zhang, H., Zhang, M., Li, Y., Wu, Y., et al. Deepseekmath: Pushing the limits of mathematical reasoning in open language models. *arXiv preprint arXiv:2402.03300*, 2024.

Slobodkin, A., Goldman, O., Caciularu, A., Dagan, I., and Ravfogel, S. The curious case of hallucinatory (un) answerability: Finding truths in the hidden states of over-confident large language models. *arXiv preprint arXiv:2310.11877*, 2023.

Tian, K., Mitchell, E., Zhou, A., Sharma, A., Rafailov, R., Yao, H., Finn, C., and Manning, C. D. Just ask for calibration: Strategies for eliciting calibrated confidence scores from language models fine-tuned with human feedback. *arXiv preprint arXiv:2305.14975*, 2023.

Tonmoy, S., Zaman, S. M. M., Jain, V., Rani, A., Rawte, V., Chadha, A., and Das, A. A comprehensive survey of hallucination mitigation techniques in large language models. *ArXiv*, abs/2401.01313, 2024.

Wei, Z., Yang, X., Sun, K., Wang, J., Shao, R., Chen, S., Kachuee, M., Gollapudi, T., Liao, T., Scheffer, N., et al. Truthrl: Incentivizing truthful llms via reinforcement learning. *arXiv preprint arXiv:2509.25760*, 2025.

Wen, B., Yao, J., Feng, S., Xu, C., Tsvetkov, Y., Howe, B., and Wang, L. L. Know your limits: A survey of abstention in large language models. *Transactions of the Association for Computational Linguistics*, 13:529–556, 2025.

Yang, A., Li, A., Yang, B., Zhang, B., Hui, B., Zheng, B., Yu, B., Gao, C., Huang, C., Lv, C., et al. Qwen3 technical report. *arXiv preprint arXiv:2505.09388*, 2025.

Yao, Z., Liu, Y., Chen, Y., Chen, J., Fang, J., Hou, L., Li, J., and Chua, T.-S. Are reasoning models more prone to hallucination? *arXiv preprint arXiv:2505.23646*, 2025.

Yu, Q., Zhang, Z., Zhu, R., Yuan, Y., Zuo, X., Yue, Y., Dai, W., Fan, T., Liu, G., Liu, L., et al. Dapo: An open-source llm reinforcement learning system at scale. *arXiv preprint arXiv:2503.14476*, 2025.

Zhang, K., Zuo, Y., He, B., Sun, Y., Liu, R., Jiang, C., Fan, Y., Tian, K., Jia, G., Li, P., et al. A survey of reinforcement learning for large reasoning models. *arXiv preprint arXiv:2509.08827*, 2025.

Zhu, X., Xia, M., Wei, Z., Chen, W.-L., Chen, D., and Meng, Y. The surprising effectiveness of negative reinforcement in llm reasoning. *arXiv preprint arXiv:2506.01347*, 2025.

## A. UCPO Extensions for Low-Resource Scenarios

In low-resource settings with restricted rollout numbers (e.g.,  $G \in [4, 8]$ ), the sparse rollout space introduces significant statistical bias and high variance. The bias arises from the coarse granularity of the probability estimates; with so few rollouts, the discrete nature of the ratios prevents  $\gamma(q)$  from spanning its full theoretical range.

As illustrated in Figure 6, the distribution of  $\gamma(q)$  for  $G = 8$  is constrained to  $[-0.354, 0.732]$ , a range significantly narrower than the theoretical extrema of  $\pm 1$ . Note that while broader values are mathematically possible, this empirical range results from the application of Non-Ternary Filtering (NTF), which excludes cases where  $P_r$  or  $P_w$  equals zero, thereby pruning the extreme tails of the theoretical discrete distribution. Such compression diminishes the reward’s discriminative power and weakens the model’s capacity to correct persistent hallucinations. Simultaneously, the limited rollout size amplifies sensitivity to individual outcomes, leading to high variance that destabilizes advantage estimation and often masks the underlying gradient. To restore the incentive’s dynamic range and ensure training stability, we extend the framework with the following strategies:

**Batch-Level Smoothing Fusion** To mitigate high variance caused by minimal group sizes, we introduce a weighted fusion mechanism that incorporates batch-level priors:

$$\gamma_{\text{fused}}(q) = \lambda \cdot \gamma_{\text{sample}}(q) + (1 - \lambda) \cdot \bar{\gamma}_{\text{batch}} \quad (6)$$

where  $\gamma_{\text{sample}}(q)$  represents the instance-specific gain and  $\bar{\gamma}_{\text{batch}}$  denotes the mean gain across the current training batch. The hyperparameter  $\lambda \in [0, 1]$  controls the trade-off between individualized response and global stability; in our implementation, we set  $\lambda = 0.5$  to achieve a balanced smoothing effect. This design effectively suppresses stochastic fluctuations while preserving the necessary sample-specific nuances required for fine-grained policy optimization.

**Non-linear Mapping Enhancement** To overcome the incentive bottleneck, we apply a hyperbolic tangent transformation to stretch the dynamic range of the gain:

$$\gamma_{\text{final}}(q) = \tanh(\alpha \cdot \gamma_{\text{fused}}(q)) \quad (7)$$

By pushing moderate gains toward the  $\pm 1$  boundaries, this mapping restores the reward signal’s ability to distinguish between varying rollout qualities, thereby overcoming a limitation frequently encountered in small-rollout settings. In our implementation with  $G = 8$ , we set the scaling factor  $\alpha = 2$  to effectively recalibrate the incentive range and maintain sufficient optimization pressure.

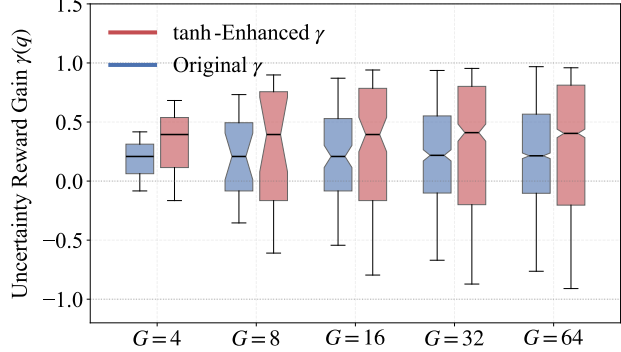


Figure 6. Impact of rollout group size  $G$  on the statistical distribution of gain  $\gamma(q)$ .

These extensions collectively allow the framework to maintain high feedback intensity and decision robustness even under severe resource constraints.

## B. Prompting Details

### {question}

Please reason step by step. If confident based on reliable knowledge, provide a clear answer and box it with `\boxed{}`.

If the question lacks clarity, exceeds your knowledge, involves speculation, prediction, opinion, or any uncertainty, do not guess. State your limitation and output `\boxed{uncertainty}`.

Figure 7. Prompt template used in Math & Text Reasoning tasks for open-ended question answering.

### {question}

Please reason step by step. If you are confident based on reliable knowledge, only output the choice letter in the answer field, e.g., answer: C.

If the question lacks clarity, exceeds your knowledge, involves speculation, prediction, opinion, or any uncertainty, do not guess. Instead, state your limitation and output uncertainty, e.g., answer: uncertainty.

Figure 8. Prompt template designed for General Tasks involving multiple-choice questions.

Figure 7 shows the prompt template used for Math & Text Reasoning tasks, where the model is guided to generate step-by-step reasoning for open-ended questions. Figure 8

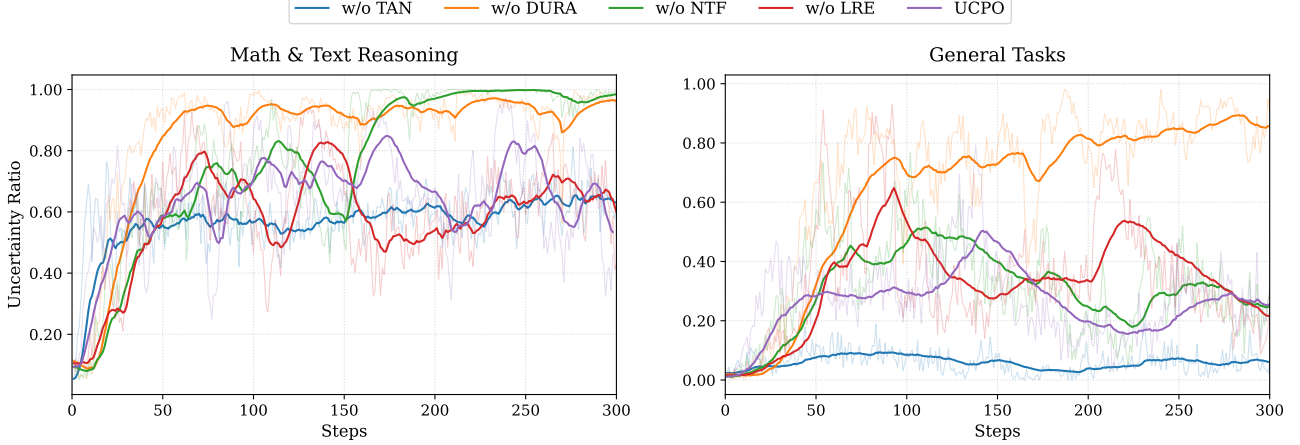


Figure 9. Training dynamics of UCPO ablation variants on Llama-3.1-8B-Instruct.

illustrates the prompt design for General Tasks, specifically multiple-choice questions, where the model selects the correct answer from given options.

## C. Additional Experimental Results

### C.1. Comparative Analysis of Ablation Study Training Processes

The training trajectories in Figure 9 provide a supplementary dynamic analysis to the ablation results presented in Section 4.4, revealing the mechanistic synergy required for stable optimization. A critical failure mode occurs upon removing DURA, where the model suffers from severe reward-hacking. In Math and Text Reasoning tasks, the model rapidly converges toward a degenerate state of near 100% uncertainty prediction to maximize reward signals. Conversely, the absence of TAD leads to erratic convergence in General Tasks because deterministic gradients overshadow the subtle signals required for calibration, causing the model to neglect uncertainty estimation entirely.

The inclusion of NTF serves as a vital regularizer for the loss landscape. While variants lacking NTF may initially converge in General Tasks, they exhibit catastrophic collapse during the later stages of Math and Text Reasoning training, highlighting the instability introduced by noisy, non-ternary samples. Regarding LRE, its contribution to long-term stability appears less definitive compared to other modules, which can be attributed to inherent variances in sample distribution and fluctuating task difficulty during the extension process. It should be noted that the scaling factors within LRE facilitate a perceptibly faster convergence in uncertainty learning by amplifying relevant advantage signals. The complex interplay between these scaling factors and data diversity warrants further exploration in future work to optimize the efficiency of metacognitive alignment.

Table 4. Performance on Llama-3.1-8B-Instruct across general tasks. Here, DAPO-UC denotes the direct addition of uncertainty as a reward term to the DAPO baseline, while DAPO-UCPO represents the full integration of our proposed UCPO framework with DAPO.

Methods	GPQA-Diamond		MMLU-Redux2		Average	
	PAQ	F1	PAQ	F1	PAQ	F1
GRPO	27.27	27.27	71.23	71.23	49.25	49.25
DAPO	34.68	34.68	74.10	74.10	54.39	54.39
GRPO-UC $\dagger^{0.5}$	34.21	18.98	78.89	71.51	56.55	45.25
DAPO-UC $\dagger^{0.5}$	33.55	22.72	77.65	75.41	55.60	49.06
UCPO	36.02	17.18	81.13	69.03	58.58	43.10
DAPO-UCPO	36.96	23.45	80.84	70.12	58.90	46.79

### C.2. Compatibility with Diverse RL Methods

UCPO is a framework-agnostic approach that can be seamlessly integrated with advanced RL methods. To demonstrate this, we extend UCPO to DAPO, which utilizes decoupled clipping and dynamic sampling to mitigate entropy collapse and enhance exploration (Yu et al., 2025). As illustrated in Table 4, we evaluate the compatibility across three comparative groups on Llama-3.1-8B-Instruct.

First, at the baseline level, DAPO exhibits a significant performance lead over GRPO (e.g., 54.39% vs. 49.25% in average PAQ), validating its superior exploration and generalization in complex reasoning. Second, when uncertainty is introduced as a simple additive reward, DAPO-UC (using the optimal coefficient of 0.5 identified in GRPO-UC) maintains better F1 scores than GRPO-UC, particularly on GPQA-Diamond (22.72 vs. 18.98), suggesting that DAPO provides a more robust policy base for uncertainty-aware rewards. Most importantly, our full integration, DAPO-UCPO, consistently achieves the best overall performance, reaching the highest average PAQ (58.90%). Notably, DAPO-UCPO

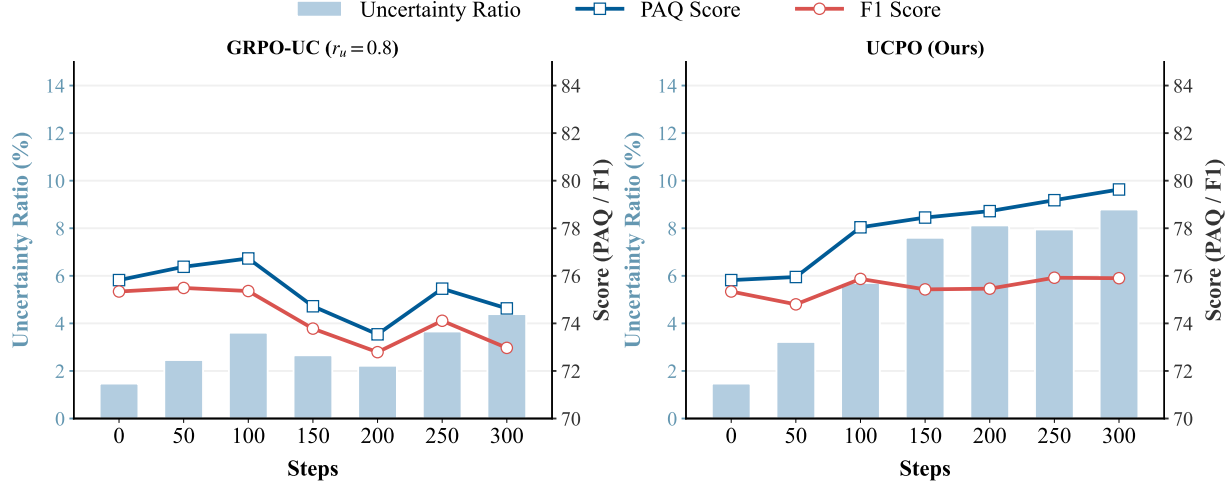


Figure 10. Average performance comparison between GRPO-UC and UCPO (Ours) on Qwen3-8B for Math & Text Reasoning tasks across different training steps.

effectively leverages DAPO’s exploration-heavy nature to complement UCPO’s calibration, resulting in a GPQA F1 score of 23.45, which is a substantial improvement over the 17.18 of vanilla UCPO. This synergy confirms that UCPO’s advantages stem from its structural optimization rather than a simple reward penalty. By leveraging the stable gradient signals and expanded policy space provided by DAPO, UCPO achieves superior calibration and generalization, demonstrating its robust compatibility across diverse preference optimization frameworks.

### C.3. Performance Comparison Across Training Steps

This section evaluates the convergence stability and performance growth trends during model fine-tuning by comparing UCPO against GRPO-UC ( $r_u = 0.8$ ), which represents the most competitive baseline configuration. The results across various models and tasks are illustrated in Figures 10, 11, 12, 13.

**Performance Trends and Comparative Gains.** Experimental results indicate that while UCPO’s PAQ scores consistently rise and then stabilize across various tasks and models, its F1 scores remain remarkably steady. This trend stems from the model’s enhanced ability to learn uncertainty representations, effectively converting previously erroneous predictions into uncertainty outputs. Notably, in the Llama-3.1-8B-Instruct math and text reasoning task, UCPO shows an initial rise in both F1 and PAQ, followed by a slight decline in the late training stage; this is likely due to the entropy collapse inherent in the GRPO algorithm, which impairs generalization. In contrast, GRPO-UC exhibits a continuous performance decline in reasoning tasks and, while showing a similar trend to UCPO in general tasks,

reaches a lower performance ceiling. This disparity highlights the significant gains UCPO derives from its dynamic adjustment mechanism.

**Mechanism of Uncertainty Evolution and Metric Trade-offs.** During the training process, the proportion of uncertainty predictions is influenced by both task difficulty and model capacity, typically following an initial growth phase that leads to an eventual plateau. Correspondingly, PAQ scores improve progressively as the model learns to identify uncertainty, while the F1 score remains stable because the potential loss in recall resulting from reclassifying low-confidence yet correct predictions as uncertainty outputs is effectively offset by significant gains in precision. By generating more precise responses with fewer hallucinations, which is the central objective of our algorithm, UCPO demonstrates superior stability and a higher performance upper bound across diverse scenarios.

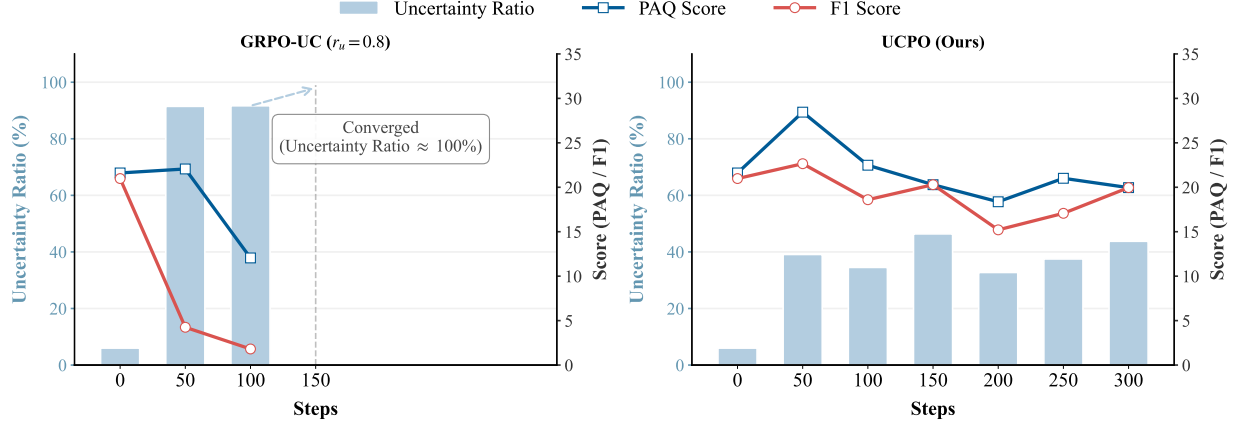


Figure 11. Average performance comparison between GRPO-UC and UCPO (Ours) on Llama-3.1-8B-Instruct for Math & Text Reasoning tasks across different training steps.

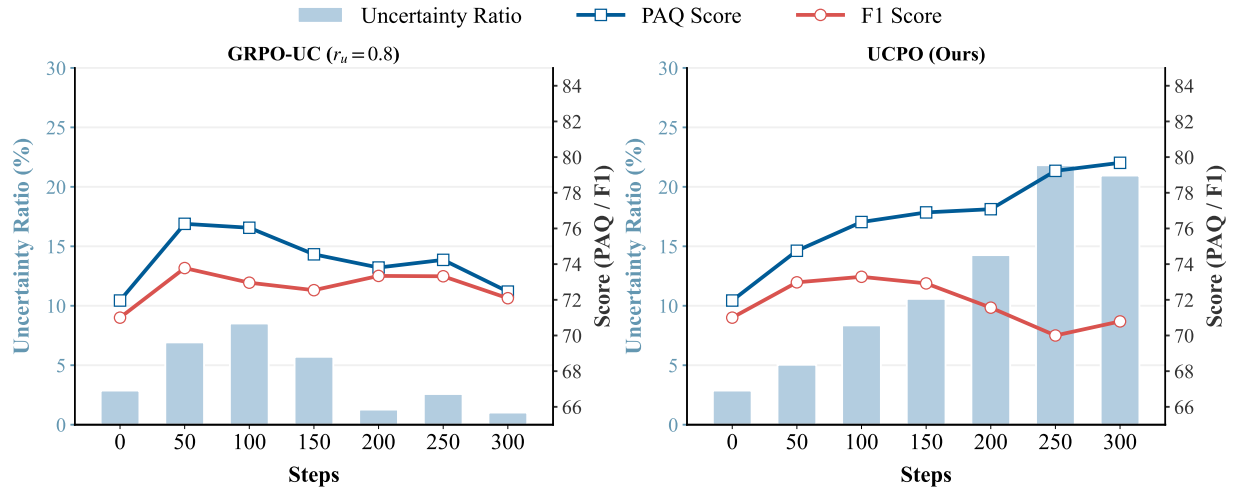


Figure 12. Average performance comparison between GRPO-UC and UCPO (Ours) on Qwen3-8B for General tasks across different training steps.

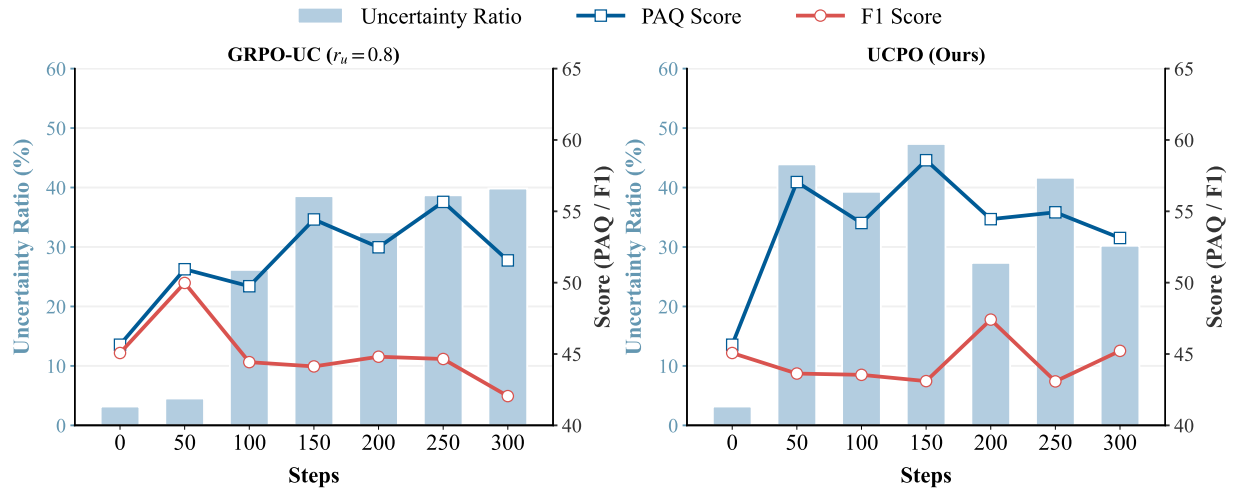


Figure 13. Average performance comparison between GRPO-UC and UCPO (Ours) on Llama-3.1-8B-Instruct for General tasks across different training steps.